Semiclassical approximations to the coherent-state propagator for a particle in a box

Ademir L. Xavier, Jr. and Marcus A. M. de Aguiar
Departamento de Física do Estado Sólido e Ciência dos Materiais, Universidade Estadual de Campinas, Caixa Postal 6165, Campinas, Brazil
(Received 30 October 1995)

We compute the semiclassical coherent-state propagator for a particle moving in a one-dimensional box. In this semiclassical approach complex trajectories are stationary paths of the propagator's asymptotic expansion and play a fundamental role. A second semiclassical approximation is also introduced, which makes use of real trajectories only. An application to a seemingly simple system, the infinite well, is carried out completely for the diagonal elements, and a comparison is made among the three possible methods, those based on complex and real trajectories and the ''exact case'' that is determined by decomposing the propagator into its eigenstates. [S1050-2947(96)04908-6]

PACS number(s): 03.65.Sq

I. INTRODUCTION

It is a remarkable fact how semiclassical methods have contributed to enlarge and clarify our understanding of quantum systems. The spirit of such semiclassical programs is to describe quantum systems by classical elements only or, at least, by classical-like elements that emerge from semiclassical approximations. The quantum postulates intrinsically describe dynamical systems by complementary schemes. These reflect themselves in the mathematical structure of the theory, which avoids conjugate variables to possess simultaneously precise measurements in a given state. A direct consequence of this fact is the nonexistence of a positive definite function with a probability interpretation associated with two conjugate variables. However, the definition of distribution functions with different physical interpretations and which depend on both conjugate parameters is possible; the Wigner [1] and Husimi [2] functions are the best examples. One very attractive application of such distributions is the possibility of a comparative study between classical phase-space structures and quantum mechanical ''phase-space'' pictures. The Husimi distribution is particularly well suited for this study, since coherent states (or Gaussian wave packets) can be regarded as the most similar probability distributions to classical particles. The connection between the Husimi and Wigner distributions is that the former can be written as a Gaussian average of the latter. This has the effect of smoothing the quantum oscillations present in the Wigner distribution and allowing the classical structures to be more easily recognized in the quantum phase-space picture.

The most natural way of introducing semiclassical approximations in quantum mechanics is through the path integral formalism developed by Feynman [3]. Its application to the usual position or momentum propagators has been studied in detail [4,5], and it has given rise, in particular, to the famous ''trace formula'' [6], which relates the density of states to a sum over periodic orbits of the corresponding classical system. The path integral version in the coherent states representation was introduced by Klauder and others [7–9], as its advantages are highly attractive, in spite of the mathematical difficulties in developing the approximation. One of these advantages, in addition to the phase-space point of view, is the freedom from caustic problems in momentum and position representations. In this work we present a brief review of the theory of the semiclassical approximation of one-dimensional coherent-state propagators as developed in detail in Ref. [12]. The main result of the theory is that the classical-like trajectories contributing to the semiclassical propagator exist in a complexified phase space and satisfy mixed end-point conditions. Of course, we expect that trajectories moving deep into the imaginary part of the phase space give exponentially small contributions and can, therefore, be neglected. The main contribution can generally be taken into account by considering only neighborhoods of real trajectories. Some recent studies [10,11] have addressed the same subject, with focus on other specific quantum systems, using, however, a different methodology. There have been several tentative schemes of complexification [13,14] in semiclassical theory recently, and some of them try to improve semiclassical formulas in the regions where the expansion by the usual stationary (real) orbits does not work properly. The inability of semiclassical relations to treat tunneling phenomena is well known, and some form of complex structure is needed, in the form of either a complex time [13] or complex trajectories [14]. The approach developed in [12] suggests a form of complexification that appears naturally as new complex dynamical equations that connect the quantum mechanical parameters (from the coherent-state propagators) to the new boundary conditions for those equations.

In this paper we apply the semiclassical formula for the coherent-state propagator to a seemingly simple system, a particle moving in a one-dimensional box. In spite of its simplicity, we shall see that this problem displays several unexpected features. In addition to the complex orbit approximation (COA) for the propagator, we also consider a real orbit approximation (ROA) where only small neighborhoods of real orbits are taken in account. Finally, we compare the results of three possible methods: the COA, the ROA, and the ''exact method,'' that is, the expansion of the propagator in its eigenstates.

This work is organized as follows: in Sec. II we review briefly the theory for the COA and ROA; in Sec. III we treat the infinite well case where complex orbits are obtained, as well as other classical elements like the energy, action etc; in Sec. IV we determine the key ingredients for the semiclassi-

cal approximation of the coherent-state propagator; and in Sec. V we present the main results and discuss conclusions and open questions.

II. BRIEF REVIEW OF THE THEORY

The quantum mechanical propagator for the time T in the coherent-state representation is defined by

$$K(z''^*,z',T)=\langle z''|e^{-\imath\hat{H}T/\hbar}|z'\rangle, \tag{1}$$

where $|z\rangle$ is the coherent state generated by the harmonic oscillator Hamiltonian $\hat{H}_0=\hat{p}^2/2+\omega^2\hat{q}^2/2$,

$$|z\rangle=e^{-1/2|z|^2}e^{za^\dagger}|0\rangle, \tag{2}$$

with $|0\rangle$ the ground state,

$$a^\dagger=\frac{1}{\sqrt{2}}\left(\frac{\hat{q}}{b}+\imath\frac{\hat{p}}{c}\right) \tag{3}$$

the creation operator, and

$$z=\frac{1}{\sqrt{2}}\left(\frac{q}{b}+\imath\frac{p}{c}\right). \tag{4}$$

The widths are given by $b=\sqrt{\hbar/\omega}$ and $bc=\hbar$. The parameters q and p that label the coherent state are real numbers.

The quantity in Eq. (1) represents the probability amplitude of a transition between the initial state $|z'\rangle$ and the final state $|z''\rangle$ after a time T. Later we will restrict the treatment to the diagonal case $z'=z''$, which is particularly important to compute the Husimi distributions of eigenstates and the spectrum. In this case we expect to find large values of $|K(z^*,z,T)|^2$ at points z close to a periodic orbit with period close to T.

A. The semiclassical propagator

A semiclassical formula for the propagator (1) has been obtained in Ref. [12] by using the path integral approach and the *steepest descent method* [15]. Here we are going to review very briefly the basic steps of this semiclassical derivation. We start, as usual, by dividing the time T into N small intervals of size ϵ and inserting into (1) $N-1$ intermediate over-completeness relations,

$$\int |z\rangle\frac{d^2z}{\pi}\langle z|=1. \tag{5}$$

In the limit where $N\to\infty$, we get

$$K(z_N^*,z_0,T)=\lim_{N\to\infty}\int\prod_{j=1}^{N-1}\frac{d^2z_j}{\pi} \times\langle z_N|e^{-\imath\hat{H}\epsilon/\hbar}|z_{N-1}\rangle\cdots\langle z_1|e^{-\imath\hat{H}\epsilon/\hbar}|z_0\rangle, \tag{6}$$

where we have set $z''=z_N$ and $z'=z_0$. Using standard properties of coherent states, Eq. (6) can be expressed in the form

$$K(z_N^*,z_0,T)=\lim_{N\to\infty}\int\prod_{j=1}^{N-1}\frac{d^2z_j}{\pi}e^{\imath\sigma/\hbar} \tag{7}$$

where

$$\sigma=\sum_{k=0}^{N-1}-\imath\hbar(z_{k+1}^*z_k-\tfrac{1}{2}|z_k|^2-\tfrac{1}{2}|z_{k+1}|^2)-\epsilon\widetilde{H}_{k+1/2} \tag{8}$$

and

$$\widetilde{H}_{k+1/2}=\frac{\langle z_{k+1}|\hat{H}|z_k\rangle}{\langle z_{z+1}|z_k\rangle}. \tag{9}$$

In the semiclassical regime ($\hbar\to0$), the integrals in Eq. (6) can be carried out by the steepest descent method. Such a procedure involves the determination of all stationary phase points, in fact a trajectory of points z_k, of σ. Not all these trajectories, however, should be included in the semiclassical approximation. Some of them are called noncontributing and should be left out; we will return to this point later.

The condition for a stationary solution reads

$$\frac{\partial\sigma}{\partial z_k}=0,\quad \frac{\partial\sigma}{\partial z_{k+1}^*}=0, \tag{10}$$

or, more explicitly,

$$\begin{aligned}&-z_k^*+z_{k+1}^*-\frac{\imath\epsilon}{\hbar}\frac{\partial\widetilde{H}_{k+1/2}}{\partial z_k}=0,\quad k=1,2,\ldots,N-1,\\ &z_k-z_{k+1}-\frac{\imath\epsilon}{\hbar}\frac{\partial\widetilde{H}_{k+1/2}}{\partial z_{k+1}^*}=0,\quad k=0,1,\ldots,N-2.\end{aligned} \tag{11}$$

In the limit $\epsilon\to0$ Eqs. (11) reduce to

$$\dot{z}=\frac{-\imath}{\hbar}\frac{\partial\widetilde{H}}{\partial z^*},\quad \dot{z}^*=\frac{\imath}{\hbar}\frac{\partial\widetilde{H}}{\partial z}, \tag{12}$$

and $\widetilde{H}(z,z^*)=\langle z|\hat{H}|z\rangle/\langle z|z\rangle$. The ''smoothed'' Hamiltonian $\widetilde{H}(z,z^*)$ does not coincide with the classical Hamiltonian $H[q(z,z^*),p(z,z^*)]$. However, the difference between the two is of order $\hbar$ and, as discussed in [12], it can be neglected in this approximation.

The solution of these equations has been discussed before, by Klauder [7] and in [12], and the key point concerns the boundary conditions. If we try to solve Eqs. (12) with $z(0)=z'$ and $z^*(T)=z^*$, we see immediately that these boundary conditions are much too restrictive for general solutions to be found. In fact, how can there be a trajectory in a two-dimensional phase space if z', z''^*, and T (five parameters) are given? The way out of this apparent conflict is given by the discrete equations (11), where we see that z_0^* and z_N never appear. Therefore, we should look for solutions of (12) with $z(0)=z'$ but $z^*(0)\neq z'^*$ and $z^*(T)=z''^*$ but $z(T)\neq z''$. General solutions satisfying the above conditions exist in a complexified phase space. Similar interpretations have been suggested in recent works [10]. Our treatment is, however, different, since we are going to directly integrate Eqs. (12).

The new complex phase space will contain stationary trajectories described by new complex parameters u and v (as substitutes for z and z^*, respectively) with

$$u=\frac{1}{\sqrt{2}}\left(\frac{q}{b}+\frac{\imath p}{c}\right),\quad v=\frac{1}{\sqrt{2}}\left(\frac{q}{b}-\frac{\imath p}{c}\right). \tag{13}$$

Note that now q and p are complex numbers and, therefore, $u\neq v^*$ in general. New Hamiltonian equations (for a complex classical mechanics) are

$$\imath\hbar\dot{u}=\frac{\partial H}{\partial v},\quad -\imath\hbar\dot{v}=\frac{\partial H}{\partial u}, \tag{14}$$

and the orbits appearing in the semiclassical propagator are those which satisfy

$$\begin{aligned} z'=u(0)=u'&=\frac{1}{\sqrt{2}}\left(\frac{q'}{b}+\frac{\imath p'}{c}\right),\\ z''^*=v(T)=v''&=\frac{1}{\sqrt{2}}\left(\frac{q''}{b}-\frac{\imath p''}{c}\right), \end{aligned} \tag{15}$$

where q', p', q'', and p'' are *real* parameters. Note also that nothing is said about the numbers u'' and v' as far as initial conditions are concerned. They are determined by the integration of the Hamiltonian equations (14) and will depend in a complicated way on u' and v''.

Expanding σ up to second order around the stationary paths and doing the quadratic Gaussian integrals gives the final coherent-state semiclassical approximation [12]

$$K_{scl}(z''^*,z',T)=\sum_j\sqrt{\frac{\imath}{\hbar}\frac{\partial^2 S_j}{\partial u'\,\partial v''}}\exp\left[\frac{\imath}{\hbar}S_j(v'',u',T)-\frac{1}{2}(|v''|^2+|u'|^2)\right], \tag{16}$$

where the sum j is performed over all possible stationary trajectories that connect the points u' and v'' in the time T, and S is the *complex action*

$$S_j(v'',u',T)=\int_0^T\left[\frac{\imath\hbar}{2}(v_j\dot{u}_j-\dot{v}_j u_j)-H(u_j,v_j)\right]dt-\frac{\imath\hbar}{2}(v''u_j''+u'v_j'). \tag{17}$$

It can be shown that the function $S_j(v'',u',T)$ obeys the relations

$$\frac{\partial S}{\partial v''}=-\imath\hbar u'',\quad \frac{\partial S}{\partial u'}=-\imath\hbar v',\quad \frac{\partial S}{\partial T}=-H, \tag{18}$$

as if u and v were conjugate variables.

Both the Hamiltonian and the action computed for such a general solution are complex numbers, and we will denote them by $H=H_1+\imath H_2$ and $S=S_1+\imath S_2$, respectively. As is easily seen, the usual classical mechanics is contained in the equations above. In fact, if

$$u(t)=v^*(t) \tag{19}$$

for $0\leqslant t\leqslant T$, a real trajectory is obtained. In this case $H_2=0$, and all variables assume real values. Also, if $z'=z''$, then this orbit is periodic with period T.

It is useful to define real phase-space variables by

$$\begin{aligned} q&=x_1+\imath p_2,\\ p&=p_1+\imath x_2. \end{aligned} \tag{20}$$

If the Hamiltonian H is an analytical function, then it is possible to write Eqs. (14) in terms of the real part $H_1(x_1,p_2,p_1,x_2)$ only and get

$$\dot{x}_1=\frac{\partial H_1}{\partial p_1},\quad \dot{p}_1=-\frac{\partial H_1}{\partial x_1},\quad \dot{x}_2=\frac{\partial H_1}{\partial p_2},\quad \dot{p}_2=-\frac{\partial H_1}{\partial x_2}. \tag{21}$$

Therefore, the one-dimensional complex dynamics can be described as a two-dimensional real mechanical system. For the sake of comparison to other results we will call Eq. (16) the *complex orbit approximation* (COA).

B. Contributing and noncontributing trajectories

The semiclassical approximation of Eq. (6) leads to the determination of all stationary trajectories satisfying Eqs. (14) and (15). There are cases, however, in which the contribution of a given stationary trajectory far exceeds the expected value of the original function, which does not correspond to any reasonable physical behavior whatsoever. To understand why these trajectories have to be excluded we recall that the semiclassical approximation treated here considers the asymptotic limit of integrals of the type

$$\mathcal{I}(\lambda)=\int_C g(z)e^{\lambda w(z)}dz, \tag{22}$$

where C is some previously defined curve and λ is a very large parameter. The steepest descent method involves the deformation of the original contour C into the steepest descent paths emanating from the stationary points (also called critical points). It so happens that some of these points may lead to a contribution larger than the very integral defined over the original contour C. When this happens such a critical point obviously cannot be taken into account in the final approximation. An outstanding simple example of a noncontributing stationary point is given by the asymptotic limit of the Airy function defined by ($n=1,2,3$)

$$F_n(s)=\frac{1}{2\pi\imath}\int_{C_n}e^{sz-z^3/3}dz,\quad w(z)=z-\frac{z^3}{3},\quad s\to\infty, \tag{23}$$

with the curves C_n defined in [15]. One of the curves (C_1) cannot be deformed into a contour emanating from the stationary point $\overline{z}=1$ simply because the resulting contribution from this point is much larger than the integrand defined over the original C_1 (see Ref. [15]). In other cases the deformation of the curve C in (22) through some stationary points is prohibited by the Cauchy theorem (see [15], p. 268, the

example of the Hankel function of type j). In all cases these stationary phase points are called *inadmissible* or *noncontributing*. There is, however, no general method which enables the direct discrimination of the noncontributing points. This determination is generally made *a posteriori*. In the process of selecting contributing and noncontributing points, not only technical but also physical arguments may be invoked in order to discriminate the anomalous outcome of inadmissible points [16].

In the case of the functional given by (6) the situation is the same (asymptotic limit for $\lambda^{-1}=\hbar\to 0$). The integration is defined over all phase space, and the complexification scheme may reveal stationary trajectories [critical points from $\sigma'(z)=0$] whose contribution is larger than the maximum value expected of $|K(z'',z,T)|$, which is 1. As every integrand entering into Eq. (6) is also limited, it follows that no stationary path which leads to a contribution larger than 1 can be taken into account in the final approximation. They are accordingly called *noncontributing trajectories*. They have also been noticed in other systems [10], and in the present system they can be easily discriminated, as we will see.

C. Example

As a simple application of the semiclassical approximation described above, we present the harmonic oscillator. As the generator of the coherent-state basis, the semiclassical approximation to the harmonic oscillator coherent-state propagator is exact. The Hamiltonian is

$$H=\frac{1}{2}p^2+\frac{\omega^2}{2}q^2 \tag{24}$$

or

$$H=\hbar\omega uv, \tag{25}$$

so that Eqs. (14) are

$$\dot{u}+\imath\omega u=0,\quad \dot{v}-\imath\omega v=0. \tag{26}$$

The complex trajectories that satisfy the boundary conditions (15) are easily determined as

$$u(t)=u'e^{-\imath\omega t},\quad v(t)=v''e^{\imath\omega(t-T)}. \tag{27}$$

Notice that $u(t)\neq v^*(t)$ in general, except in the special case where $u'=v''^*$ and $T=2n\pi/\omega$. The action is

$$S(v'',u',T)=-\imath\hbar u'v''e^{-\imath\omega T}, \tag{28}$$

and the propagator is finally given by

$$K(z''^*,z',T)=\exp\left[-\frac{\imath\omega T}{2}+z'z''^*e^{-\imath\omega T}-\frac{1}{2}(|z''|^2+|z'|^2)\right]. \tag{29}$$

D. Approximation by real trajectories

Complex trajectories have complex actions. If S_2 is positive the trajectories give an exponentially small contribution to the semiclassical propagator. We would then expect that only slightly complex orbits give a substantial contribution and a quadratic expansion around real orbits would retain the essential information. Assuming that the classical motion is bounded, we see that through each phase-space point (q,p) with $H(q,p)=E$ (one degree of freedom) there is a periodic orbit with period $\tau=\tau(E)$. Therefore, as discussed in [12], if T is close to τ, i.e.,

$$T=\tau+\delta T, \tag{30}$$

an expansion of the action is possible:

$$S(z^*,z,T)\simeq S(z^*,z,\tau)+\frac{\partial S}{\partial T}\delta T+\frac{1}{2}\frac{\partial^2 S}{\partial T^2}\delta^2 T. \tag{31}$$

The coefficients of this expansion can be calculated with the help of Eqs. (18) and give

$$\frac{\partial S}{\partial T}=-H(u',v')=-E_0, \tag{32}$$

$$\frac{\partial^2 S}{\partial T^2}=-\frac{\partial H}{\partial T}=-\frac{\partial H}{\partial v'}\frac{\partial v'}{\partial T}=-\frac{\imath}{\hbar}\frac{\partial H}{\partial v'}\frac{\partial^2 S}{\partial u'\,\partial T}, \tag{33}$$

where E_0 is the energy of the real orbit around which the approximation is made. Using also the relation

$$H\left(\frac{\imath}{\hbar}\frac{\partial S}{\partial v''},v''\right)=-\frac{\partial S}{\partial T} \tag{34}$$

and differentiating both sides with respect to u', we can further simplify (33) and get

$$\frac{\partial^2 S}{\partial T^2}=-\dot{u}\dot{v}\frac{\partial^2 S}{\partial u'\,\partial v''}=-\alpha. \tag{35}$$

Substituting these approximations into (16) we find

$$\widetilde{K}_{scl}(z^*,z,T)=\sum_j\sqrt{\frac{\imath}{\hbar}\frac{\partial^2 S(z^*,z,\tau_j)}{\partial u'\,\partial v''}}\exp\left[\frac{\imath}{\hbar}S_j(z^*,z,\tau_j)-|z|^2-\frac{\imath}{\hbar}E_0\delta T-\frac{\imath}{2\hbar}\alpha\delta T^2\right], \tag{36}$$

which we call the real orbit approximation (ROA).

As we will see in the explicit example of a particle in a box, Eq. (36) does provide a good approximation to the propagator for most values of q, p, and T.

In the next sections we will compute the propagator for a particle moving in a box of an infinite square-well potential according to the three available methods: the complex orbit approximation, the real orbit approximation, and by expanding the propagator in its eigenstates:

$$K(z''^*,z',T)=\sum_{n=1}^{\infty}\langle z''|n\rangle\langle n|z'\rangle e^{-\imath E_nT/\hbar} \tag{37}$$

where $|n\rangle$ is the eigenstate

$$\langle x|n\rangle=\left(\frac{2}{L}\right)\sin\left(\frac{n\pi x}{L}-\frac{n\pi}{2}\right),\quad n=1,2,3,\ldots, \tag{38}$$

whose energy is

$$E_n=\frac{\hbar^2\pi^2n^2}{2L^2}. \tag{39}$$

We call the propagator determined by (37) the *exact case* since it will work as the standard quantum calculation to which semiclassical methods will be compared. In Eq. (37), the Husimi functions are determined by

$$\langle n|z\rangle=\left(\frac{1}{\sqrt{\pi}b}\right)^{1/2}\int_{-\infty}^{\infty}\langle n|x\rangle \times\exp\left[-\frac{(x-q)^2}{4b^2}+\frac{\imath}{\hbar}p(x-q/2)\right]dx. \tag{40}$$

Since the infinite sum in Eq. (37) is not numerically treatable, it is necessary to introduce a cutoff. Our numerical calculations for the exact propagator (see Sec. V) include up to 400 eigenstates, so as to make the square value of the modulus of $K(z^*,z,0)$ very close to 1 for most of the phase-space region under study.

III. THE INFINITE WELL SYSTEM

The infinite well system is described by the Hamiltonian function

$$H(q,p)=\begin{cases}\dfrac{p^2}{2}, & |x|\leqslant\dfrac{L}{2},\\[2ex] \infty, & |x|>\dfrac{L}{2}.\end{cases} \tag{41}$$

Although this Hamiltonian is not analytical, it can be seen as a limit of an analytic set of Hamiltonians of the form

$$H_n(q,p)=\frac{p^2}{2}+\left(\frac{2q}{L}\right)^{2n} \tag{42}$$

for $n\to\infty$ and the real equations (20) and (21) may be applied. Therefore, the associated two-dimensional Hamiltonian is given by

$$H_1(x_1,p_2,p_1,x_2)=\begin{cases}\dfrac{1}{2}(p_1^2-x_2^2), & x_1^2+p_2^2\leqslant\dfrac{L^2}{4},\\[2ex] \infty, & x_1^2+p_2^2>\dfrac{L^2}{4}.\end{cases} \tag{43}$$

The system is then transformed into a circular infinite well where the particle bounces in a particular way against the potential walls. The boundary conditions (15) imply the following bonds on the solutions of the system (21):

$$\begin{aligned} x_1(0)-x_2(0)&\equiv x_1'-x_2'=q',\\ p_1(0)+p_2(0)&\equiv p_1'+p_2'=p',\\ x_1(T)+x_2(T)&\equiv x_1''+x_2''=q'',\\ p_1(T)-p_2(T)&\equiv p_1''-p_2''=p'', \end{aligned} \tag{44}$$

where q', p', q'', p'', and T are given, and we have set $c=b=1$. We will specifically treat wave packets of minimum uncertainty throughout this work.

A. Integration

According to (21), the equations of motion are given by

$$\begin{aligned} \dot{x}_1&=p_1, \quad \dot{x}_2=0,\\ \dot{p}_1&=0, \quad \dot{p}_2=x_2, \end{aligned} \tag{45}$$

and a straightforward integration yields

$$\begin{aligned} x_1(t)&=\frac{T(q''-q')+2(p''+p')}{4+T^2}t+q'\\ &\quad+\frac{2(q''-q')-T(p''+p')}{4+T^2},\\ p_2(t)&=\frac{2(q''-q')-T(p''+p')}{4+T^2}t+p'\\ &\quad-\frac{T(q''-q')+2(p''+p')}{4+T^2},\\ x_2(t)&=\frac{2(q''-q')-T(p''+p')}{4+T^2},\\ p_1(t)&=\frac{T(q''-q')+2(p''+p')}{4+T^2}. \end{aligned} \tag{46}$$

We call solutions (46) *direct trajectories*, since no bounce occurs in the interval $0\leqslant t\leqslant T$. It must, however, be emphasized that relations (15) do not automatically lead to the also necessary conditions

$$|x_1'|\leqslant\frac{L}{2}, \quad |p_2'|\leqslant\frac{L}{2}, \quad |x_1''|\leqslant\frac{L}{2}, \quad |p_2''|\leqslant\frac{L}{2} \tag{47}$$

that are applied independently in order to sort out the correct solutions from the general ones.

Reflection at the boundary gives rise to a change in the sign of the complex momentum,

$$p_1\to-p_1, \quad x_2\to-x_2, \tag{48}$$

since the complex energy is a constant of motion. We call n the trajectory *order*, which is equal to the total number of bounces during the time evolution. If $\overline{x_1^{(j)}}$ and $\overline{p_2^{(j)}}$ are the points where the jth collision occurs at the time t_j, the particle position and momentum are

$$\begin{aligned} p_1^{(j+1)}(t)&=(-1)^jp_1', \quad x_1^{(j+1)}(t)=p_1^{(j+1)}(t-t_j)+\overline{x_1^{(j)}},\\ x_2^{(j+1)}(t)&=(-1)^jx_2', \quad p_2^{(j+1)}(t)=x_2^{(j+1)}(t-t_j)+\overline{p_2^{(j)}}, \end{aligned} \tag{49}$$

for $t_j\leqslant t\leqslant t_{j+1}$. The collision points are related by the *border relation*

$$\overline{x_1^2}+\overline{p_2^2}=\frac{L^2}{4}. \tag{50}$$

The relations between two successive reflections are

$$\overline{x_1^{(j+1)}}=p_1^{(j+1)}\Delta+\overline{x_1^{(j)}},$$
$$\overline{p_2^{(j+1)}}=x_2^{(j+1)}\Delta+\overline{p_2^{(j)}}, \tag{51}$$
$$\Delta=t_j-t_{j-1}.$$

It is easy to see that every possible solution can be classified according to two main types depending on the sign of the final momentum: *even trajectories* (n even) and *odd trajectories* (n odd). The final momentum is therefore

$$p_1''=(-1)^n p_1',$$
$$x_2''=(-1)^n x_2'. \tag{52}$$

Relations (44) enable us to write connection formulas for the initial and final positions. We easily find that, for even trajectories,

$$x_1''=p_1'(T-n\Delta)+x_1',$$
$$p_2''=x_2'(T-n\Delta)+p_2', \tag{53}$$

and for odd trajectories,

$$x_1''=-p_1'[T+\Delta(n-1)-2t_n]+x_1',$$
$$p_2''=-x_2'[T+\Delta(n-1)-2t_n]+p_2'. \tag{54}$$

By substituting relations (44) in (53) and (54), the complex momentum is easily found. For n even ($n\geqslant 2$),

$$p_1'^{(n)}=\frac{(T-n\Delta)(q''-q')+2(p''+p')}{4+(T-n\Delta)^2},$$
$$x_2'^{(n)}=\frac{2(q''-q')-(T-n\Delta)(p''+p')}{4+(T-n\Delta)^2}, \tag{55}$$

and for n odd ($n\geqslant 1$),

$$p_1'^{(n)}=\frac{q''-q'}{2t_n-T-\Delta(n-1)},$$
$$x_2'^{(n)}=-\frac{p''+p'}{2t_n-T-\Delta(n-1)}. \tag{56}$$

This is but a partial calculation, since p_1 and x_2 still depend on the collision time t_n and on Δ, which are found with the help of relation (50). We only need to have suitable relations for $\overline{x_1}$ and $\overline{p_2}$. These come from the last bounce (even trajectories, $n\geqslant 2$)

$$\overline{x_1^{(n)}}=q''-x_2'-p_1'(T-t_n),$$
$$\overline{p_2^{(n)}}=p_1'-p''-x_2'(T-t_n), \tag{57}$$

and (odd trajectories, $n\geqslant 1$)

$$\overline{x_1^{(n)}}=q''+x_2'+p_1'(T-t_n),$$
$$\overline{p_2^{(n)}}=x_2'(T-t_n)-p_1'-p''. \tag{58}$$

Since two variables (Δ and t_n) must be determined, two equations are required. Applying relation (50) again for the $(n-1)$th collision gives (even trajectories, $n\geqslant 2$)

$$\overline{x_1^{(n)}}=q''-x_2'-p_1'^{(n)}(T-t_n-\Delta),$$
$$\overline{p_2^{(n)}}=p_1'-p''-x_2'^{(n)}(T-t_n-\Delta), \tag{59}$$

and (odd trajectories, $n\geqslant 1$)

$$\overline{x_1^{(n)}}=q''+x_2'+p_1'^{(n)}(T-t_n-\Delta),$$
$$\overline{p_2^{(n)}}=x_2'^{(n)}(T-t_n-\Delta)-p_1'-p''. \tag{60}$$

Next we are going to analyze these solutions according to their order and determine equations for the time variables in (55) and (56). We will specifically treat diagonal elements, so that from now on we will restrict the former equations to the case $q'=q''=q$ and $p'=p''=p$.

B. Analysis of complex trajectories

1. n=0

For $n=0$ there is no bounce, but Eqs. (47) limit the phase-space region where a direct trajectory can be found. In general, these solutions are found in regions of low momentum and for small times T. They also dominate the phase space for $T\to 0$. Applying relations (47) to the direct trajectories (46), we get the existence conditions

$$T^2p^2+4pqT-B^2(4+T^2)<0,$$
$$T^2p^2-4pqT-B^2(4+T^2)<0, \tag{61}$$

with

$$B^2=\frac{L^2}{4}-q^2. \tag{62}$$

Figure 1 shows an example (for $T=1.0$) of the existence regions in phase space for even and odd trajectories with several orders. The $n=0$ region is the first shaded area around the line $p=0$.

2. n=1

If we define $\xi_1=2t_1-T$ and apply Eqs. (58) in (50) we easily get

$$B^2\xi_1^2+4pq\xi_1-(4+T^2)p^2=0 \tag{63}$$

which immediately gives

$$t_1=\frac{T}{2}+\frac{1}{4B^2}[4pq\pm|p|\sqrt{L^2(4+T^2)-4q^2T^2}]. \tag{64}$$

3. n even (≥2)

If we substitute Eqs. (57) and (59) in relation (50) and use the definitions

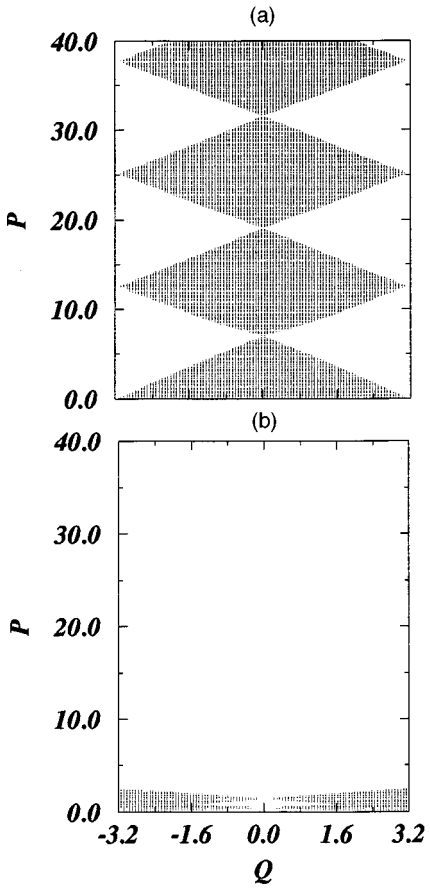

FIG. 1. The dashed area shows the phase-space regions where diagonal real and complex orbits [with $u'(0)=z$ and $v''(T)=z^*$] for $T=1.0$ can be found: (a) trajectories with n even ($n=0$ in the first half diamond, $n=2$ in the second diamond, etc.); (b) trajectories with n odd from $n=1$ to $n=5$.

$$\xi_n=2t_n-T-n\Delta,$$
$$\xi_{n-1}=2t_n-T-(n-2)\Delta, \tag{65}$$
$$\alpha_n=T-n\Delta,$$

two quadratic equations are obtained:

$$p^2\xi_n^2+4pq\xi_n-B^2(4+\alpha_n^2)=0,$$
$$p^2\xi_{n-1}^2+4pq\xi_{n-1}-B^2(4+\alpha_n^2)=0. \tag{66}$$

Since the coefficients in Eqs. (66) are the same and the solutions are

$$\xi^{\pm}=-\frac{2q}{p}\pm\frac{1}{|p|}\sqrt{L^2+\alpha_n^2B^2} \tag{67}$$

we take $\xi_n=\xi^+$ and $\xi_{n-1}=\xi^-$. By definition (65) we have

$$(\xi_{n-1}-\xi_n)^2=4\Delta^2, \tag{68}$$

which results, together with (67), in a quadratic equation for Δ:

$$\Delta^2(B^2n^2-p^2)-2B^2n\Delta+L^2+B^2T^2=0. \tag{69}$$

It is easy to see that Eq. (69) contains among its solutions the real one. In this particular case $\alpha_n=0$, and it gives

$$\Delta=\frac{L}{|p|}. \tag{70}$$

The general solutions are

$$\Delta^{\pm}=\frac{B^2nT\pm\sqrt{(p^2-B^2n^2)L^2+p^2T^2B^2}}{B^2n^2-p^2}. \tag{71}$$

The last bounce time t_n is calculated by summing $\xi_n+\xi_{n-1}$, or

$$t_n=\frac{1}{2}\left[T+\Delta(n-1)-\frac{2q}{p}\right]. \tag{72}$$

4. n odd ($\geqslant 3$)

Again we substitute Eqs. (58) and (60) in (50) with the definition

$$\xi_n=\xi_{n-1}=2t_n-T-\Delta(n-1) \tag{73}$$

and a pair of equations is also obtained:

$$B^2\xi_n^2+4pq\xi_n-\{4+[T-\Delta(n-1)]^2\}p^2=0,$$
$$B^2\xi_{n-1}^2+4pq\xi_{n-1}-\{4+[T-\Delta(n+1)]^2\}p^2=0. \tag{74}$$

Given (73), possible solutions exist if

$$[T-\Delta(n-1)]^2=[T-\Delta(n+1)]^2; \tag{75}$$

that is $\Delta=0$ or $\Delta=T/n$. Taking the only reasonable solution

$$\Delta=\frac{T}{n}, \tag{76}$$

we find by summing $\xi_n^{\pm}+\xi_{n-1}^{\pm}$ that

$$t_n=\frac{1}{2}\left[T\left(\frac{2n-1}{n}\right)+\frac{1}{2}(\xi_n^{\pm}+\xi_{n-1}^{\pm})\right] \tag{77}$$

with

$$\xi_n^{\pm}+\xi_{n-1}^{\pm}=-\frac{4pq}{B^2}\pm\frac{2|p|}{B^2}\sqrt{L^2+\left(\frac{BT}{n}\right)^2}. \tag{78}$$

However, it must be pointed out that general solutions for t_n and Δ are still limited by the ''causal'' requirement

$$0<\Delta<t_n<T. \tag{79}$$

The number of solutions will strongly depend on the parameters q, p, and T. While odd trajectories for a given p (low), q, and T may present a multitude of possible solutions (several orders), even trajectories in general are unique in n for small values of T. The phase space is also far from being completely covered by complex orbits. In semiclassical terms the regions of phase space that lack complex trajectories are related to very low probability transition amplitudes. In fact, we will see that for such regions the semiclassical approximation is zero. Figure 1 shows the regions of exist-

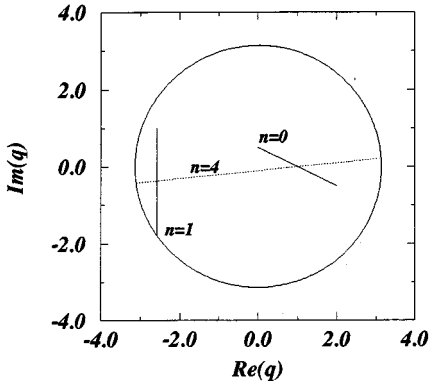

FIG. 2. Complex diagonal trajectories for $T=1.0$ in the x_1-p_2 plane. The $n=0$ trajectory has $q=1.0$ and $p=2.5$; $n=1$, $q=1.0$, and $p=1.0$; and $n=4$, $q=1.0$, and $p=21.0$. The circle represents the potential boundary.

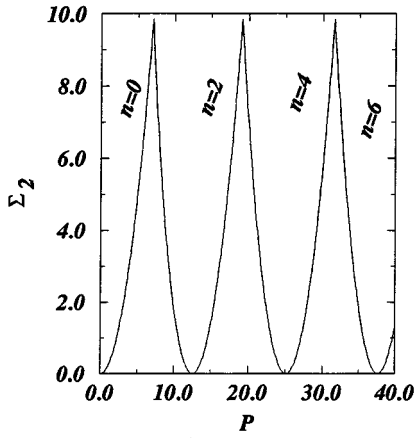

FIG. 3. Imaginary part of the phase Σ_2 as a function of p for $q=0$ and $T=1.0$. When $\Sigma_2=0$, the momenta take real values according to $p=nL/p$.

ence of solutions for even trajectories and odd trajectories when $T=1.0$. We see that odd trajectories are limited to a small area around $p=0$, and solutions of several orders exist for some points in phase space. On the other hand even trajectories are restricted to diamond shaped areas for each order. As the value of p increases the number of bounces increases accordingly. In Fig. 2 are shown some examples of trajectories for $T=1.0$ in the complex q plane together with the well boundary. The $n=0$ trajectory corresponds to a direct orbit with end points $q=1.0$ and $p=2.5$. The odd trajectory $n=1$ has $q=1.0$ and $p=1.0$ and the even orbit $n=4$ has $q=1.0$ and $p=21.0$.

IV. THE PROPAGATOR

We now proceed to the determination of the COA, Eq. (16). According to Eq. (15), we can write

$$u''^{(n)}=v''+\sqrt{2}\imath(-1)^n p^{(n)},$$
$$v'^{(n)}=u'-\sqrt{2}\imath p^{(n)}, \tag{80}$$

with $n=0,1,2,\ldots$, $p^{(n)}=p_1^{(n)}+\imath x_2^{(n)}$, and $u'=v''^*$ (diagonal elements). For the infinite well system (and also for quadratic one-dimensional systems) the action does not contain the integral part, so that

$$S_n(v'',u',T)=-\frac{\imath\hbar}{2}[v''u''^{(n)}+u'v'^{(n)}] \tag{81}$$

or by (80)

$$S_n(v'',u',T)=-\frac{\imath\hbar}{2}\{u'^2+v''^2+\imath\sqrt{2}p^{(n)}[-u'+(-1)^n v'']\} \tag{82}$$

is the complex action for the infinite well.

A direct substitution of the trajectories in the argument of the exponential in (16) shows that, for odd trajectories, it may happen that

$$\Sigma_2=\mathrm{Im}\left[S_n(v'',u',T)+\frac{\imath\hbar}{2}(|v''|^2+|u'|^2)\right]<0, \tag{83}$$

which implies an abnormal increase in the final amplitude $[|K(z^*,z,T)|^2\propto\exp(-\Sigma_2)\gg 1]$. This unexpected behavior is related to the problem of noncontributing stationary trajectories (see Sec. II B) and they should not enter into the final semiclassical approximation. In fact, we will see that the contribution from direct trajectories is indeed enough for a good approximation in phase-space regions of low momentum (in Fig. 1 the area of odd trajectories shrinks to the line $p=0$ as $T\to\infty$). In the following analysis we will, therefore, consider even trajectories only, since they dominate almost all the phase space.

For direct trajectories, and consequently the $n=0$ region, the semiclassical approximation is analytically given by

$$K_{scl}(z^*,z,T)=(1+\imath\beta T)^{-1/2}\exp\left[\frac{\imath\beta T p^2}{1+\imath\beta T}\right] \tag{84}$$

with $\beta=1/4$.

The behavior of Σ_2 (83) as function of p at $q=0$ is depicted in Figs. 3 and 4 for $T=1.0$ and $T=12.0$, respectively, in the case of even trajectories. The imaginary part of the

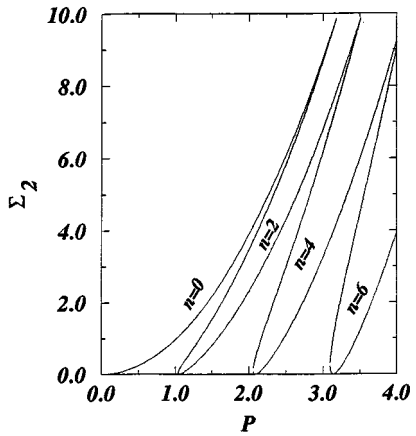

FIG. 4. Imaginary part of the phase Σ_2 as a function of p for $q=0$ and $T=12.0$. As T increases, several orbits with different orders can contribute to the same phase point z.

phase Σ_2 goes to zero at the real orbit, and assumes positive values for complex orbits. This shows that the propagator amplitude is maximal at the real orbits and goes smoothly to zero outside them. For low momentum, as T increases, several orders can contribute to the amplitude, which means semiclassically that several semiclassical paths exist connecting the initial and final states.

We still have to determine the amplitude or second variation of the action $\partial^2 S/\partial u' \partial v''$. Starting with Eq. (18),

$$-\imath\hbar v' = \frac{\partial S}{\partial u'}, \tag{85}$$

and using (80), it gives

$$\frac{\partial^2 S}{\partial u' \partial v''} = -\hbar \left[\left(\frac{\partial p_1^{(n)}}{\partial q''} - \frac{\partial x_2^{(n)}}{\partial p''} \right) + \imath \left(\frac{\partial x_2^{(n)}}{\partial q''} + \frac{\partial p_1^{(n)}}{\partial p''} \right) \right] \Bigg|_{q,p}. \tag{86}$$

The derivatives in relation (86) require the determination of the collision times for general elements ($q' \neq q''$ and $p' \neq p''$); the final derivatives must then be calculated at the diagonal elements. It is then straightforward to get

$$\begin{aligned}
\left. \frac{\partial p_1}{\partial q''} \right|_{q,p} &= \frac{\alpha_n}{4+\alpha_n^2} - \frac{8\alpha_n p}{(4+\alpha_n^2)^2} \left. \frac{\partial \alpha_n}{\partial q''} \right|_{q,p}, \\
\left. \frac{\partial p_1}{\partial p''} \right|_{q,p} &= \frac{2}{4+\alpha_n^2} - \frac{8\alpha_n p}{(4+\alpha_n^2)^2} \left. \frac{\partial \alpha_n}{\partial p''} \right|_{q,p}, \\
\left. \frac{\partial x_2}{\partial q''} \right|_{q,p} &= \frac{2}{4+\alpha_n^2} - \left[\frac{2p}{4+\alpha_n^2} - \frac{4\alpha_n^2 p}{(4+\alpha_n^2)^2} \right] \left. \frac{\partial \alpha_n}{\partial q''} \right|_{q,p}, \\
\left. \frac{\partial x_2}{\partial p''} \right|_{q,p} &= -\frac{\alpha_n}{4+\alpha_n^2} - \left[\frac{2p}{4+\alpha_n^2} - \frac{4\alpha_n^2 p}{(4+\alpha_n^2)^2} \right] \left. \frac{\partial \alpha_n}{\partial p''} \right|_{q,p},
\end{aligned} \tag{87}$$

with α_n given in Eqs. (65) and

$$\left. \frac{\partial \alpha_n}{\partial q''} \right|_{q,p} = \frac{2pq\alpha_n^2 + 4(q^2+2p^2)\alpha_n}{\alpha_n p(4B^2 - p^2/n^2) - 8p^2(2q + pT/n^2)},$$

$$\left. \frac{\partial \alpha_n}{\partial p''} \right|_{q,p} = -\frac{2(B^2 - 2p^2/n^2)\alpha_n^2 + 4p(2pT/n^2 - 7q)\alpha_n + 8q^2 + 4[2B^2 - (pT/n)^2]}{p\alpha_n(4B^2 - p^2/n^2) - 8p^2(2q + pT/n^2)}. \tag{88}$$

Equations (82) and (86) to (88) determine the semiclassical propagator completely. In the next section we are going to compare the ''exact'' with the real and complex orbit approximations.

V. RESULTS AND CONCLUSION

In order to present some numerical comparisons between the exact result, the COA, and the ROA, we have fixed $L = 2\pi$, $\hbar = 1$, and also the coherent-state widths $b = c = 1$. To compute the ROA for the propagator at the phase point z and time T, we first find the real orbit through this point. If τ_0 is its period, we take its mth repetition such that $|T - m\tau_0|$ is as small as possible. The final expression in this case is

$$|\tilde{K}_{scl}(z^*, z, T)|^2 = \left| \frac{\partial^2 S}{\partial u'' \partial v'}(q,p,\tau) \right| \exp\left[\frac{\imath}{2\hbar}(\alpha^* - \alpha)\delta T^2 \right],$$

$$\alpha = |\dot{u}|^2 \frac{\partial^2 S}{\partial u'' \partial v'}(q,p,\tau), \tag{89}$$

$$\delta T = T - \tau, \quad \tau = m\tau_0.$$

Figures 5 to 7 show contour plots of $|K(z^*, z, T)|^2$ for $T = 0.5$, 1.0, and 1.5, respectively. In each of these figures we show the exact result, the COA, and the ROA. These figures show a probability concentration around periodic trajectories, corresponding to the fact that the amplitude expresses the correlation between the initial quantum state represented by $|z\rangle$ and the final state $|z, T\rangle$. In the vicinity of a periodic orbit, clearly $|z\rangle \sim |z, T\rangle$ and the amplitude exhibits a large value. As T increases, the number of periodic orbits with period proportional to T grows accordingly, so that the number of ''scars'' of periodic orbits in the quantum phase-space maps also increases. From the comparison of the three approximations we see that the COA (b) has a q dependence which is not present in the ROA (c). This dependence disappears in the real approximation, because the same real orbit is used to approximate the amplitude in every phase-space point in the q line. Since this periodic orbit is characterized by the momentum only, the set of points near it will assume the same amplitude. The p dependence is otherwise given by the exponential in (89).

The most important difference between the ROA and the COA is the lack of probability amplitude near the line $p = 0$ for the real approximation. The COA uses direct complex trajectories in this region, as we have already discussed. In fact, the number of distinct orbits used in the ROA is much smaller than in the COA where, for each phase-space point, there is a different complex trajectory.

As far as the absolute probability amplitude is concerned, the good agreement of the semiclassical procedures with the exact propagator can be appreciated in Fig. 8, where we show $|K(z^*, z, T)|^2$ as function of p for $q = 0$. Parts (a), (b), and (c) show results for $T = 0.5$, 1.0, and 1.5, respectively, with solid lines representing the amplitude as calculated by the COA, while circles display the ROA, and dot-dashed lines represent the exact propagator. The widths of the semi-

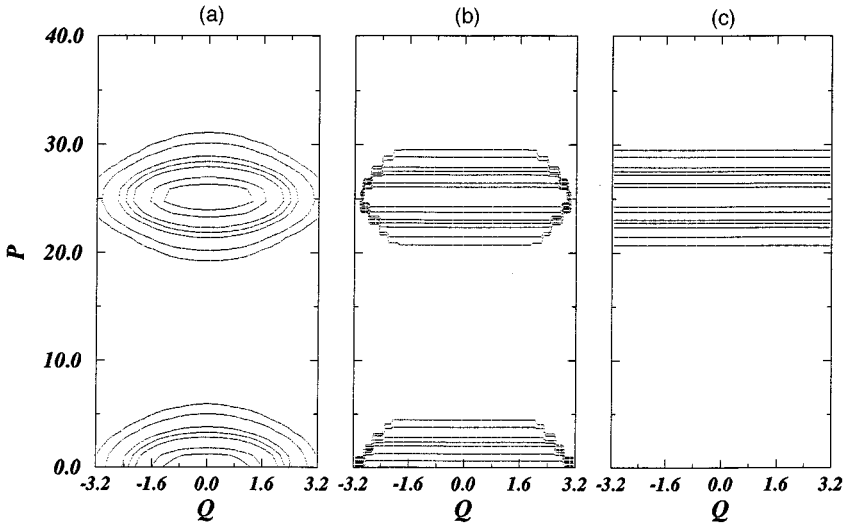

FIG. 5. Contour plots of $|K(z^*,z,T)|^2$ (normalized) for $T=0.5$: (a) the exact case, (b) the complex approximation (COA), and (c) the ROA.

classical approximations are slightly smaller than those given by the exact propagator. Figures 9 and 10 show $|K(z^*,z,T)|^2$ versus q at fixed values of p. In Fig. 9 we have chosen $p=1.125$, such that the orbits contributing to K never hit the potential boundary $(n=0)$, while in Fig. 10 we have chosen p such that the orbits hit the boundary twice $(n=2)$. In both figures parts (a), (b), and (c) show results for $T=0.5$, $T=1.0$, and $T=1.5$, respectively (notice that Fig. 9 does not show the ROA, which is zero for $n=0$). From these figures we see that the q dependence of the COA interpolates between the maximum and minimum values reached by the smooth exact propagator, although it is very abrupt.

From the results presented in this paper, we see that the semiclassical methods are very successful in describing the infinite well potential, for which the poorest agreement would in principle be expected due to the discontinuity of the potential. We believe that the results should improve for smoother potentials. This system was treated at a ''semianalytical'' level, that is, we have developed analytically the main relations as far as possible, and then numerical calculation was used. It is not difficult to see that a similar treatment of other potentials is hardly possible, and then numerical methods must be applied thoroughly. We have already developed a numerical algorithm to compute complex orbits satisfying the necessary boundary conditions in a generic one-dimensional situation. The method and its application to a smooth potential will be presented elsewhere.

Our calculations also point out an important result: contrary to our initial expectations, it is not true that there is always a complex orbit from $u(0)=u'$ to $v(T)=v''$ in the time T for all u', v'', and T. For a fixed T, at the phase-space regions where such orbits do not exist, the semiclassical propagator is zero. From the numerical results, we see that this is, however, not critical, since the exact propagator itself is very small at these places. On the other hand, complexification is thought to save semiclassical methods from their inability to treat some dynamical systems where real trajectories may not exist. Now, we have seen an example where, for a great part of the phase-space, even complex trajectories do not exist.

Another interesting result of the paper was the computation of odd trajectories, assembled around the line $p=0$. These were seen to result in a nonphysical contribution to the propagator at this line because they exceed the limiting value of $K(z^*,z,T)$. From a more physical point of view, we notice that the even trajectories are the natural analytical continuation of the real periodic orbits. The odd trajectories, on the other hand, possess no physical interpretation whatso-

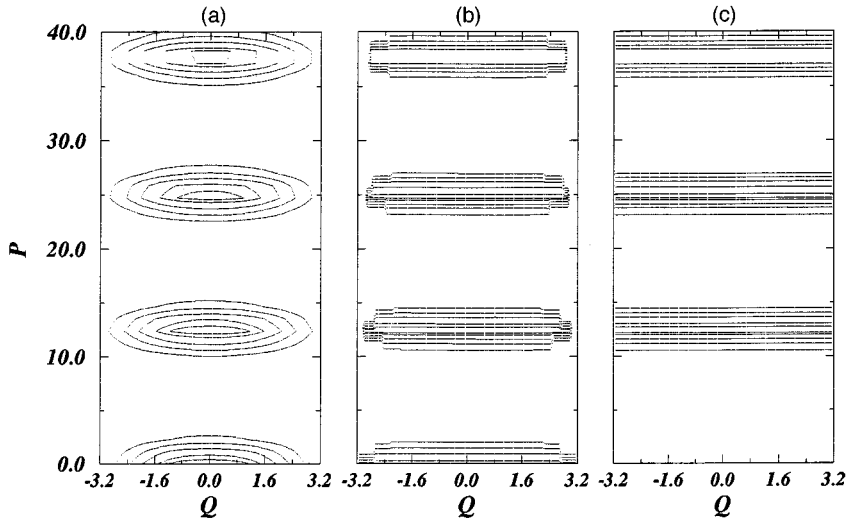

FIG. 6. Contour plots of $|K(z^*,z,T)|^2$ (normalized) for $T=1.0$: (a) the exact case, (b) the complex approximation (COA), and (c) the ROA.

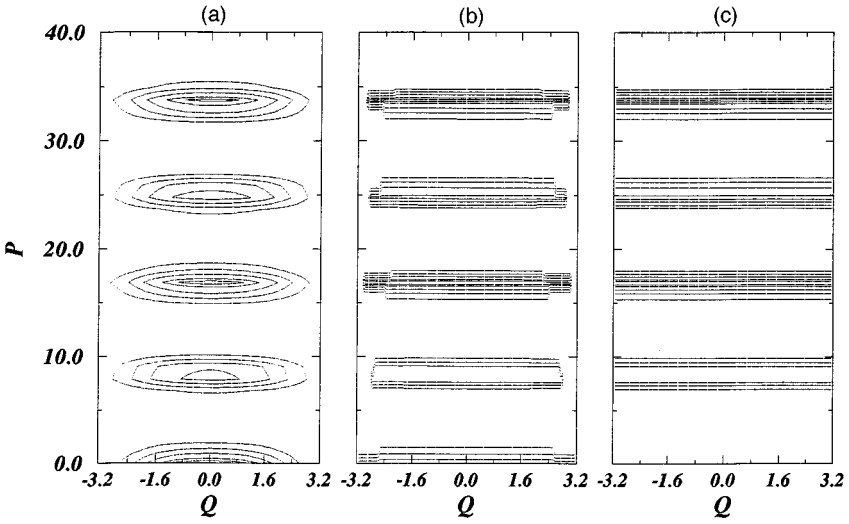

FIG. 7. Contour plots of $|K(z^*,z,T)|^2$ (normalized) for $T=1.5$: (a) the exact case, (b) the complex approximation (COA), and (c) the ROA.

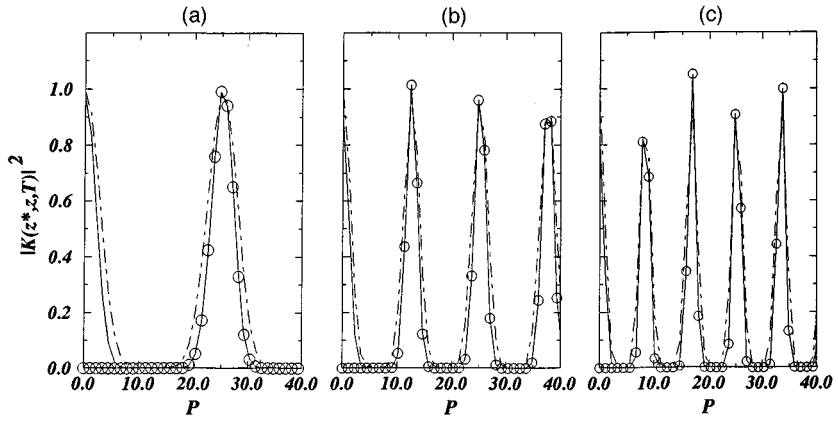

FIG. 8. Absolute value of $|K(z^*,z,T)|^2$ at $q=0$: (a) $T=0.5$, (b) $T=1.0$, and (c) $T=1.5$. Solid line is the COA, dot-dashed line represents the exact propagator, and circles the ROA.

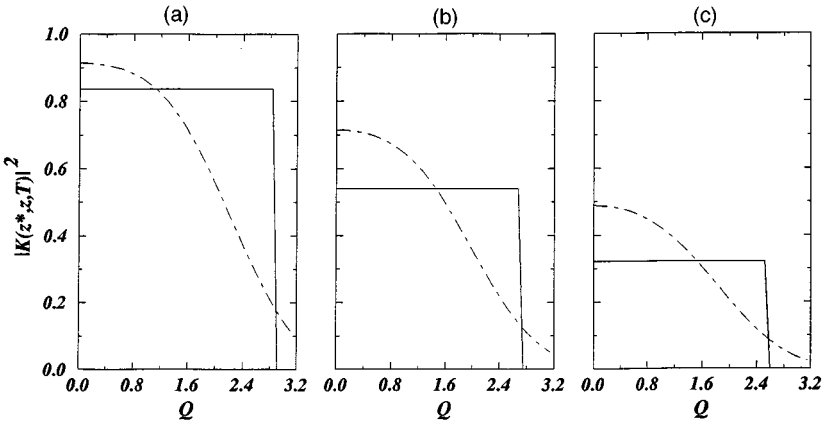

FIG. 9. Absolute value of $|K(z^*,z,T)|^2$ at $p=1.125$ $(n=0)$ for different times: (a) $T=0.5$, (b) $T=1.0$, and (c) $T=1.5$. Solid line represents the COA and dot-dashed line the exact propagator.

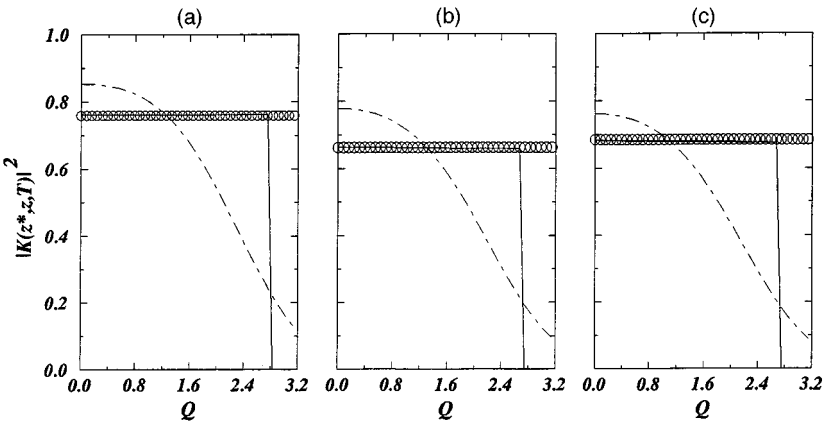

FIG. 10. Absolute value of $|K(z^*,z,T)|^2$ for $n=2$ for different times: (a) $T=0.5$ and $p=23.62$, (b) $T=1.0$ and $p=13.5$, and (c) $T=1.5$ and $p=9.0$. Solid line represents the COA, dot-dashed line the exact case, and circles the ROA.

ever. Indeed, a real trajectory with initial (q,p) that bounces just once at the wall has its momentum changed in sign and can never return to the same phase-space point before bouncing again at the opposite wall. In this sense odd trajectories are unphysical and should be discarded. This conclusion is also justified *a posteriori*, since the contributions from direct trajectories totally account for the propagator for $p \simeq 0$.

The application of complex semiclassical dynamics to nondiagonal elements of the propagator is also possible, though more complicated. Such a calculation would enable the study of the time evolution of Gaussian wave packets, with complex trajectories connecting phase-space points not accessible by real dynamics (they would connect different parts of the propagated packet). Suggestive as it seems, tunneling effects, in particular, could be studied in this way.

ACKNOWLEDGMENTS

The authors would like to acknowledge financial support from CNPq, FAPESP, and FINEP. One of the authors (A.L.X.J.) specially acknowledge support from FAPESP (Fundação de Amparo à Pesquisa do Estado de São Paulo), Contract No. 93/2490-0.

[1] E. Wigner, Phys. Rev. **40**, 749 (1932).
[2] K. Husimi, Proc. Phys. Math. Soc. Jpn. **22**, 264 (1940).
[3] R. P. Feynman and A. R. Ribbs, *Quantum Mechanics and Path Integrals* (McGraw-Hill, New York, 1965).
[4] J. H. Vleck, Proc. Natl. Acad. Sci. U.S.A. **140**, 178 (1928).
[5] C. Morette, Phys. Rev. **81**, 848 (1951).
[6] M. C. Gutzwiller, *Chaos in Classical and Quantum Mechanics* (Springer-Verlag, New York, 1990).
[7] J. R. Klauder, in *Path Integrals*, Proceedings of the NATO Advanced Study Institute, edited by G. J. Papadopoulos and J. T. Devreese (Plenum, New York, 1978), p. 5.
[8] J. R. Klauder, Phys. Rev. D **19**, 2349 (1979)
[9] Y. Weissman, J. Phys. A **16**, 2693 (1983).
[10] S. Adachi, Ann. Phys. (N.Y.) **195**, 45 (1989).
[11] A. Robin and J. R. Klauder, Ann. Phys. (N.Y.) **241**, 212 (1995).
[12] M. A. M. de Aguiar and M. Baranger (unpublished).
[13] D. W. McLaughlin, J. Math. Phys. **13**, 1099 (1972).
[14] K. Takatsuka and H. Ushiyama, Phys. Rev. A **51**, 4353 (1995).
[15] N. Bleistein and R. A Handelsmann, *Asymptotic Expansion of Integrals* (Dover, New York, 1969).
[16] A. Erdélyi, *Asymptotic Expansions* (Dover, New York, 1956).